

https://dspace.org/

Experimental Investigation on the Effect of Gold Tailings as a Partial Replacement for Sand in Concrete

Jacob Ikotun; Rhoda Adeyeye; Mike Otieno

https://hdl.handle.net/10539/43605
WOS

Downloaded from a DSpace repository. https://dspace.org/

sustainability

MDPI

Article

Experimental Investigation on the Effect of Gold Tailings as a Partial Replacement for Sand in Concrete

Jacob O. Ikotun [1,*], Rhoda A. Adeyeye [1,*] and Mike Otieno [2]

[1] Department of Civil Engineering, Durban University of Technology, Pietermaritzburg 3209, South Africa
[2] School of Civil Engineering and Environmental Engineering, University of the Witwatersrand, Johannesburg 2050, South Africa; mike.otieno@wits.ac.za
* Correspondence: jacobi@dut.ac.za (J.O.I.); 22172827@dut4life.ac.za (R.A.A.)

Abstract: This study explores the use of secondary gold tailings (SGTs) in concrete production to solve sand sustainability issues. This approach addresses waste issues and presents a sustainable material alternative to conventional sand, investigating different SGT proportions (ranging from 0% to 100%) to replace fine aggregate in structural concrete. This study examined the fresh, mechanical, and durability properties of concrete containing SGTs. Incorporating SGTs reduced the concrete's workability, but up to a 75% replacement level resulted in a high fresh concrete density compared with the reference concrete. The results indicated that up to 25% replacement level increased the compressive strength and up to 50% replacement level improved the splitting tensile strength compared with reference concrete. However, all concretes containing SGTs exhibited satisfactory strengths. The statistical analysis confirmed the significant influence of SGTs on concrete strength. In addition, the durability results of the concrete demonstrated good resistance to oxygen, water, and chloride penetration, indicating good concrete quality. SGTs are recommended as a substitute for crusher sand to reduce production costs, conserve natural resources, and promote a sustainable and greener environment.

Keywords: secondary gold tailings; concrete; workability; compressive strength; oxygen permeability; water sorptivity

check for updates

Citation: Ikotun, J.O.; Adeyeye, R.A.; Otieno, M. Experimental Investigation on the Effect of Gold Tailings as a Partial Replacement for Sand in Concrete. *Sustainability* **2024**, *16*, 7762. https://doi.org/10.3390/su16177762

Academic Editor: Miguel Bravo

Received: 26 July 2024
Revised: 29 August 2024
Accepted: 30 August 2024
Published: 6 September 2024

Copyright: © 2024 by the authors. Licensee MDPI, Basel, Switzerland. This article is an open access article distributed under the terms and conditions of the Creative Commons Attribution (CC BY) license (https://creativecommons.org/licenses/by/4.0/).

1. Introduction

Concrete is an important construction material because of its strength, durability, and versatility. It comprises cement, aggregate, water, and admixture, with aggregate constituting 65–80% of its volume. Notably, fine aggregate accounts for around 30% of the aggregate, indicating its substantial use in concrete production [1,2]. Fine aggregate (sand) is important in mortar and concrete production, playing a key role in mix design [3]. The properties and proportion of fine content in sand significantly impact the concrete composition [4]. Sand contributes a mass of particles capable of resisting applied loads, ensuring prolonged durability compared with cement paste alone. Thus, sand assumes a crucial role in enhancing the solidification and strength of concrete [5]. Sand influences the relationship between cement paste and aggregates [4]. It fills the pores between coarse aggregate particles, stabilizing concrete mixtures. This results in well-packed particles and good bonding within the concrete matrix, impacting fresh concrete properties and the strength and durability of hardened concrete [6]. The properties of the sand determine the surface texture of concrete, influencing the concrete's interface with construction materials [7]. Since sand is an important component of concrete, its sustainability is worthy of consideration.

The sustainability of sand in concrete production poses a challenge. Natural sand used for concrete production is extracted from natural deposits like rivers, dunes, alluvial plains, and beaches. Relentless extraction due to the extensive use of sand in concrete production

depletes natural sand reserves and natural sand regeneration is insufficient to offset the extraction rate. Furthermore, sand mining disrupts ecosystems, lowers water tables, causes erosion, alters topography, and destroys vegetation [8]. Therefore, to sustain the supply of sand for concrete production, the construction industry has turned to quarrying natural rock, producing manufactured sand or crushed sand. However, producing crushed sand from natural rock consumes 3.0 × 106 GJ of energy and releases 260 × 106 Kg CO_2, adding to greenhouse gas emissions [9]. In addition, it causes pollution, landscape destruction, and disruption of local biota [10]. To address sand production problems, researchers in the construction field have proposed using solid waste as a partial or full substitute for sand [11]. Solid wastes investigated as sand substitutes for producing sustainable concrete include iron lathes, glass waste, and waste foundry sand [12–14].

Tailings are solid waste from mining, produced when extracting valuable minerals from ores. Globally, rapid industrial growth has increased annual tailings production. South Africa produces 315 million tons annually, with 105 million tons from gold extraction, resulting in over 1.7 billion tons of stockpiled gold tailings [15–18]. As mining activities have rapidly increased, high-grade ore deposits have steadily decreased. The gold mine grade is projected to decline from 3–4 g/t in 2012 to 1 g/t by 2050 [19]. Some stockpiled gold tailings in South Africa are being reprocessed to recover the remaining minerals and further reduce their toxic substances. This generates "secondary gold tailings", finer grains stacked up without a noticeable decrease in the tailings volume, as shown in Figure 1 [15,20]. Research has demonstrated that effective metals and other useful components can be recovered from gold tailings, using combined floatation processes [21]. Moreover, the levels of toxic substances in gold tailings that undergo further processing are lower than those that do not [22]. Therefore, some expected oxides and metals in reprocessed gold tailings (secondary gold tailings) might be lower in content or absent. However, the land disposal of tailings poses issues [23]. It leads to pollution, costly construction, and constant maintenance, consumes extensive land, and negatively impacts nearby mining areas economically [24]. Tailings, a challenge in the mining industry, now demand efficient use for sustainable mining growth. Their properties, including paste fluidity and mechanical behavior, make them viable for engineering and construction materials [25,26]. Research has explored their potential as concrete aggregates, emphasizing the crucial need to repurpose them for industrial advancement [27].



Figure 1. Stockpiled secondary gold tailings from the Fairview Mine in Barberton, Mpumalanga, South Africa.

Similar to other types of tailings, gold tailings have the potential to substitute sand to produce sustainable concrete. Reddy et al. [28] found that replacing up to 30% river sand with gold tailings improved concrete strength. Preethi et al. [29] reported that 20% river sand replacement with gold tailings produced suitable strength, advocating for their use in concrete to conserve sand, reduce pollution, and promote environmentally friendly and economical practices. Ahmed et al. [30] utilized 60% gold tailings in place of quartz sand in ultra-high-performance concrete and noticed increased strengths and reduced water absorption. Their findings indicate that gold tailings enhance the strength of concrete, are eco-friendly, and are cost-effective when utilized in mining environments. Balegamire et al. [31] observed similar compressive strengths in concrete with river sand and with gold tailings. They proposed using gold tailings as a sand replacement for better living conditions in mining areas. Song et al. [32] reported that substituting up to 40% river sand with gold tailings improved concrete's strength and durability in terms of water absorption and chloride ion permeability, with the best performance at a 30% substitution level. They concluded that substituting river sand with gold tailings in concrete can reduce the dependence on river sand, significantly improving resource sustainability.

Most of the research has predominantly examined the strength performance of concrete made with gold tailings, overlooking durability [27]. Durability properties such as oxygen permeability index, water sorptivity index, and the chloride conductivity index of concrete containing gold tailings have not been reported in the literature. These properties are good indicators of the durability performance of concrete and are worthy of consideration. Furthermore, previous research has focused on using gold tailings as a substitute for river sand, while their use as a replacement for manufactured sand in concrete has rarely been documented. Additionally, the utilization of secondary gold tailings as a sand substitute in concrete has not been reported. Therefore, this study aims to advance sustainable growth in the construction and mining sectors by using secondary gold tailings (SGTs) to replace crusher sand in the production of green concrete. The investigation examined the fresh, mechanical, and durability properties of the concrete.

2. Experimental Work

2.1. Materials

In this study, SGTs and andesite crusher sand served as fine aggregates; their visual appearance is shown in Figure 2. SGTs were collected from the Fairview Mine in Barberton, Mpumalanga, South Africa. Andesite crusher sand was procured from the Afrisam Plant in Johannesburg, South Africa; its manufacturer specifications complied with SANS 1083:2014 [33]. The physical properties of the two fine aggregates such as density, fineness modulus, water absorption, and particle size distribution were assessed consecutively according to the South African Standard [34,35]. The density test was performed using a pycnometer density analyzer. A weighed empty pycnometer was filled with fine aggregate, weighed, and recorded. The test was run at room temperature, and measurement values were recorded automatically after the pycnometer containing fine aggregate was placed into the density analyzer apparatus connected to a gas cylinder.

The particle size distribution of the fine aggregates was determined by sieve analysis. The fine aggregate was poured into a nest of stacked sieves with a size of 4.75 mm at the top and 0.075 mm at the bottom, installed in a mechanical sieve shaker. After shaking the sieve for 15 min with the mechanical sieve shaker, the fine aggregate was separated into size fractions based on sieve apertures. The fine aggregates retained on each sieve and the one in the sieve receiver were weighed and recorded. The fineness modulus of the fine aggregates was obtained using sieve analysis. Additionally, the water absorption test was conducted using the pycnometer. The saturated surface dried of fine aggregate of a specific weight was poured into the weighed pycnometer, which was then filled with water. The mixture was stirred to eliminate air voids and the pycnometer containing the mixture was weighed and recorded. The fine aggregate was transferred to a clean container with a known weight after water removal. The fine aggregate in the container was oven-dried for

24 h at 100 °C. The oven-dried fine aggregate was measured and recorded, and the water absorption was computed using Equation (1).

$$\% \, Abs = \frac{M_S - M_D}{M_D} \times 100 \quad (1)$$

where Abs represents the water absorption, M_S represents the mass of the saturated surface-dried fine aggregate, and M_D represents the mass of the oven-dried fine aggregate.



Figure 2. The visual appearance of secondary gold tailings and andesite crusher sand.

Also, the mineral composition of the fine aggregates was investigated using X-ray diffraction (XRD). This was performed using a Malvern Panalytical Aeris with a PIXcel detector and Fe-filtered Co-Kα radiation. The sample was tested at a step size of 0.02° at a scanning rate of 0.5 s/step. The X'Pert Highscore plus software identified the phases and the Rietveld method was used to estimate the relative phase amounts (weight %). Scanning electron microscopy (SEM) was used to examine the chemical composition and microstructure of the fine aggregates. This was conducted using the ZEISS Merlin FE SEM device. The device combines ultra-fast analytics with high-resolution imaging, enabling a wide range of beam flexibility from a voltage of 20 V to 30 kV and beam currents of 7 pA to 40 nA. An energy-dispersive X-ray (EDX) unit installed on the device was used to analyze the elemental composition of the fine aggregates. The results of the examined properties are presented in Section 3.

In this study, plain Portland cement (PC) of strength class 52.5 (CEM I 52.5 R) was utilized. This cement was sourced from the Afrisam Plant in Johannesburg, South Africa, and the manufacturer's specification conformed with SANS 50197-2:2011 [36]. Type C fly ash was used as a cement extender, with the manufacturer's specifications following SANS 50450-1:2014 [37]. A Sika ViscoCrete 3088 superplasticizer, composed of an aqueous solution of modified polycarboxylate conforming to BS EN 934-2:2009 [38], was utilized to enhance the workability of the mixture without the need for additional water. In addition, tap water was used as mixing water. In this study, andesite crushed stone of size 19 mm (uniformly graded) was used as a coarse aggregate. The material was sourced from the Afrisam Plant, Johannesburg, South Africa, and the manufacturer's specifications followed SANS 1083:2014 [33].

2.1.1. Mixture Proportion

The concrete mixture proportions were determined using the volumetric mix design method established by the Cement and Concrete Institute (C&CI) in South Africa, to design a reference concrete of strength grade 35 MPa. As shown in Table 1, six mixtures were prepared with a constant water–cement ratio of 0.5. The concrete slump considered in the design ranged from 75 to 150 mm. Quantities of water, crushed stone, cement, and fly ash remained constant across the mixture proportions. A constant 70–30% blend of

plain Portland cement and fly ash (PC-FA) was used, chosen based on South African practice and supported by previous studies showing satisfactory durability and strength performance [39].

Table 1. Mix proportions for 1 m^3 of concrete samples.

Mix Label	Binders (kg/m^3)		Aggregates (kg/m^3)			Water (kg/m^3)	W/C	SP Dosage (%)
	PC	FA	Andesite Crushed Stone (Uniformly Graded 19 mm Size)	Andesite Crusher Sand	Secondary Gold Tailings			
GT0	294	126	1084	842	-	210	0.5	0.06
GT10	294	126	1084	757.8	84.2	210	0.5	0.078
GT25	294	126	1084	631.5	210.5	210	0.5	0.85
GT50	294	126	1084	421.0	210	210	0.5	1.23
GT75	294	126	1084	210.5	631.5	210	0.5	1.58
GT100	294	126	1084	-	842	210	0.5	1.96

Andesite crusher sand and SGT proportions varied across mixture proportions, depending on the replacement levels of 0%, 10%, 25%, 50%, 75%, and 100% of the crusher sand volume. Designations GT0, GT10, GT25, GT50, GT75, and GT100 denote the concrete mixture proportions, with GT0 representing the reference concrete in this study. SGTs replaced the andesite crusher sand according to the listed replacement levels. The replacement levels were at 25% intervals. The 10% replacement level was included to determine the behavior of concrete containing a small portion of SGTs. Also, the superplasticizer (SP) doses varied from 0.06% to 1.96% of the cement weight, determined according to the SGT content in the mixes.

2.1.2. Specimen Preparation

Based on the mix design, six batches of concrete mixture proportions were prepared within a temperature range of 22 °C to 25 °C, conforming to SANS 5861-1:2006 [40]. The six batches of concrete were designated as GT0, GT10, GT25, GT50, GT75, and GT100, respectively. GT0 was the first batch, representing the reference concrete. GT0 contained only andesite crusher sand, while the remaining five batches contained varying portions of SGTs based on the replacement levels. The dry materials were mixed for 1 min, followed by continuous mixing with water and superplasticizer for another 1 min. Subsequently, the slump and fresh concrete density tests were conducted. After the tests, cubic specimens ($100 \times 100 \times 100$ mm^3 were cast for the mechanical properties and durability tests. After 24 h, specimens were demolded and cured in water at 22 °C to 25 °C until 7, 28, 56, and 90 days of curing, for subsequent testing.

2.2. Fresh Concrete Tests

The slump test was carried out for each of the concrete proportions following SANS 5862-1:2006 [41], using a slump cone with dimensions of 300 mm height, 100 mm top diameter, and 200 mm base diameter. Also, the fresh concrete density was measured and calculated for each concrete proportion, in conformity with SANS 6250:2006 [42].

2.3. Compressive Strength and Splitting Tensile Strength Tests

Specimens' compressive strength and splitting tensile strength were determined using a cube press-foot CTE 56-1216 FTP compression testing machine and an Amsler compressive strength testing machine of capacity 2000 kN, respectively. The tests were conducted in conformity with SANS 5863:2006 [43] and SANS 6253:2006 [44], respectively with a testing speed set at 0.3 MPa/s. For each test, three specimens from each mixture proportion at curing ages of 7, 28, 56, and 90 d were tested, taking the average strengths as the test results.

2.4. Durability Tests

Durability tests were conducted on the specimens, based on the South African durability index (DI), namely, oxygen permeability, water sorptivity, and chloride conductivity. The DI assessed the quality of the concrete specimens regarding the transport of gas, moisture, and chloride after 28, 56, and 90 days of curing, complying with South African standards for the procedures [45]. Concrete discs with a diameter of 70 ± 2 mm and a thickness of 30 ± 2 mm cut from 100 × 100 × 100 mm^3 specimens were used for the three tests. The preparation of concrete discs from a concrete sample is shown in Figure 3. Four concrete discs from each mixture proportion at each curing day were tested for each DI test. The average values of each DI measurement were recorded as the test results. The concrete discs were subjected to a temperature of 50 ± 2 °C for 7 days in the oven and cooled to 23 ± 2 °C before being used for the tests. Four specimens per mixture proportion were tested for each DI after each curing age.



Figure 3. Preparation of sample concrete disc for durability tests.

2.4.1. Oxygen Permeability Index Test

The oxygen permeability index test was carried out after each curing age, in conformity with South African standards [45]. Figure 4 shows oxygen permeability index testing. Each concrete disc was placed in the permeability cell, and oxygen was released into the cell until the pressure in the cell reached 100 ± 5 kPa. Subsequently, the data logging devices automatically recorded the pressure value at 15 min intervals until the pressure in the cell was reduced to 50 ± 2.5 kPa or until 6 h ± 15 min had elapsed. Based on the pressure and time results, oxygen permeability was calculated as the negative logarithm of the coefficient of permeability [45].



Figure 4. Oxygen permeability cell setup.

2.4.2. Water Sorptivity Index Test

The water sorptivity index test assessed the concrete's porosity and water absorption rate after each curing age, in conformity with South African standards [45]. Water sorptivity index testing is presented in Figure 5. The concrete discs were sealed at the curved sides, weighed, and the measurements recorded. Afterward, the discs were placed on paper towels in a tray containing calcium hydroxide solution at 23 ± 2 °C. The unsealed face in contact with the solution was limited to a 2 mm height above the disc side. The discs were periodically weighed at 3, 5, 7, 9, 12, 16, 20, and 25 min intervals within 10 s of their removal while still in a saturated and dry-surface condition. The concrete discs were vacuum sealed at 75 kPa for 3 h ± 15 min, followed by soaking in calcium-saturated water for 1 h ± 15 min with no air penetration in the vacuum saturation tank, restoring the vacuum to 75 kPa. The vacuum was released, and the specimens were soaked in the air that penetrated the tank for 18 ± 1 h. Then, the specimens were saturated dry and weighed. The porosity of each concrete disc was calculated using Equation (2):



Figure 5. Water sorptivity testing of concrete samples.

$$n = \frac{M_{sv} - M_{s0}}{Adp_w} \times 100 \quad (2)$$

where n represents porosity, M_{sv} represents the mass of the concrete disc saturated with a vacuum (g), M_{s0} represents the mass of the concrete disc at the start of the experiment (g), A represents the concrete disc's cross-sectional area (mm), d represents the average thickness of the concrete disc (mm), and p_w represents water density (g/mm).

The water sorptivity for each concrete disc was calculated using Equation (3) [45]:

$$S = \frac{Fd}{M_{sv} - M_{s0}} \quad (3)$$

where S represents the water sorptivity of the concrete discs, F represents the best-fit line's slope (g/$\sqrt{}$h), d represents the average thickness of the specimens (mm), M_{sv} represents the mass of the concrete disc saturated in a vacuum (g), and M_{s0} represents the mass of the concrete disc at the start of the experiment (g).

2.4.3. Chloride Conductivity Index

The chloride conductivity index test assessed concrete porosity and chloride diffusion after each curing age, in conformity with South African standards [45]. The chloride conductivity testing of a concrete sample is shown in Figure 6. Concrete discs were sealed in vacuum saturation at 75 kPa for 3 h ± 15 min. After that, the specimens were immersed in sodium chloride (NaCl) for 1 h ± 15 min without air exposure in the vacuum saturation tank, restoring the vacuum to 75 kPa. The vacuum was released, and the specimens were soaked in air that penetrated the tank, for 18 ± 1 h. Then, the specimens were saturated dry, weighed, and placed in a chloride cell with 5 M NaCl in both chambers consecutively. Using a 10 V DC power supply, current and voltage were measured simultaneously via an ammeter and voltmeter. The chloride conductivity for each disc was calculated using Equation (4) [45]:

$$\sigma = \frac{id}{VA} \quad (4)$$

where σ represents the specimen's chloride conductivity (mS/cm), i represents electric current (mA), d represents the concrete disc's mean thickness (cm), V represents voltage difference (V) and A represents the cross-sectional area of the concrete disc.

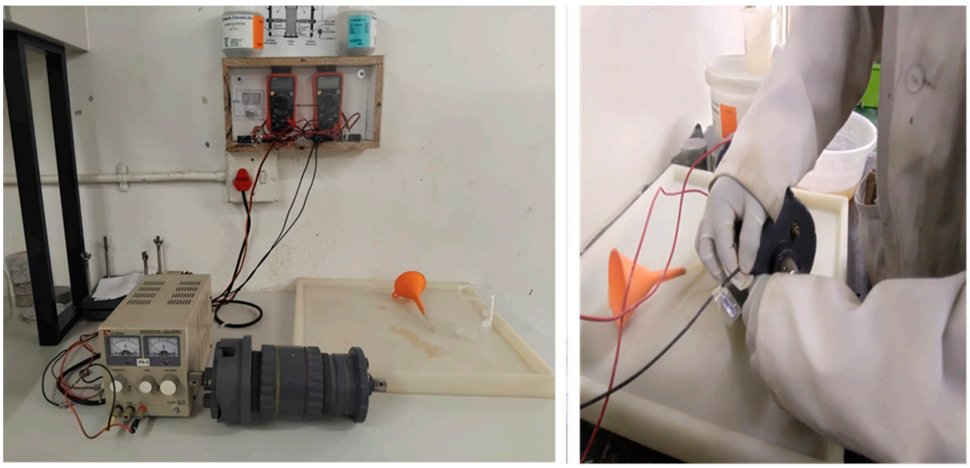


Figure 6. Chloride conductivity testing of concrete samples.

3. Results and Discussion

3.1. SGT and Andesite Crusher Sand Characterization

The elemental compositions of SGTs and andesite crusher sand are presented in Table 2, indicating that SGTs had a higher SiO_2, Al_2O_3, and K_2O content than andesite crusher sand.

This is attributed to the higher percentages of Si, K, Al, and O in SGT, resulting from the presence of muscovite [46,47]. The absence of Na, Ca, Cl, and S indicates the absence of Na_2O, CaO, ClO_2, and SO_3 in the SGTs. However, these oxides were found in the gold tailings used in studies by Mashifana and Sithol [22], Chen et al. [19], and Song et al. [32], indicating that reprocessing of gold tailings led to the absence of these oxides in SGTs. Moreover, CaO, which usually participates in hydration reactions, was absent in SGTs in the current study, suggesting that these SGTs might not generate extra calcium silicate hydrate (C-S-H) in concrete [48]. However, CaO was found in the gold tailings used in the study by Song et al. [32], generating more hydration products. Also, the absence of SO_3 and ClO_2 in SGTs suggests that the SGTs are relatively inert. The absence of some oxides in SGTs suggests that some metals and other useful components have been recovered from the gold tailings used in this study.

Table 2. The elemental composition of secondary gold tailings and crusher sand.

Element	Percentage by Weight of Secondary Gold Tailings (%)	Percentage by Weight of Andesite Crusher Sand (%)
Si	20.96	8.78
Fe	0.54	2.56
Al	8.11	1.58
Mg	0.35	0.8
Na	0.00	0.4
K	8.06	0.56
O	59.33	42.34
Ca	0.00	26.58
Cl	0.00	0.1
S	0.00	0.58
C	2.65	15.76

Gold tailings where gold had been further recovered were alkaline and posed no threat of acidic discharge [49]. This suggests that SGTs generated from reprocessed gold tailings are alkaline, as confirmed by the absence of acidic sulfides in SGTs, and poses no risk of leaching. This is consistent with the findings in the study by Ahmed et al., [30] which reported that gold tailings had lower concentrations of heavy metals than the permissible limit, attributed to their alkaline nature. According to Mashifana and Sithol [22], the gold tailings used in their study were further processed, and it was reported that gold tailings posed no risk of heavy metals leaching due to low concentrations of heavy metals compared with the regulatory limits. This indicates that SGTs have low concentrations of heavy metals, leading to the conclusion that SGTs pose no threat of leaching heavy metal.

Furthermore, according to the XRD results for SGTs presented in Figure 7, the minerals present in the SGTs were quartz (SiO_2), albite [$NaAlSi_3O_8$], microcline [$KAlSi_3O_8$], and soft minerals such as muscovite [$Kal_2(AlSi_3O_{10})(F,OH)_2$], dolomite [$CaMg(CO_3)_2$], siderite [$FeCO_3$], and clinochlore [$(Mg,Fe^{2+})_5Al_2Si_3O_{10}(OH)_8$] [30]. The XRD patterns indicated a high level of quartz, predominately silicate. This finding is consistent with the research by Mashifana and Sithol [22], where quartz had the highest peak intensity in gold tailings. The high quartz composition was due to its dominance in the original gold tailings and high resistance to physical and chemical weathering and dissolution. The host rock in the Barberton area, where the current sample was collected, contains up to 50% quartz [22]. This contributed to the high quartz content detected in the SGTs used in this study. The SGTs had high muscovite content (14%), which might be concentrated in fine particles of SGTs, resulting from gold tailings reprocessing [50]. The results showed that gypsum in the SGTs was negligible, explaining the negligibility or absence of CaO in the SGTs.

Pyrite content is usually found in gold tailings, because gold ore bodies are associated with pyrite [21,22]. However, pyrite mineral was not detected in the SGTs used in this study, indicating its recovery during reprocessing. The absence of pyrite in the SGTs suggests that the SGTs were inert, with no threat of leachability. Pyrite is a sulfide mineral and its absence explains the negligibility of sulfide in the SGTs, as shown in Table 2 [51]. In addition, uranium was not detected in the SGTs, indicating that the SGTs were non-radioactive. Also, the SEM images of the SGTs and crusher sand, shown in Figure 8, show that both fine aggregates had an angular shape and a porous, rough surface.

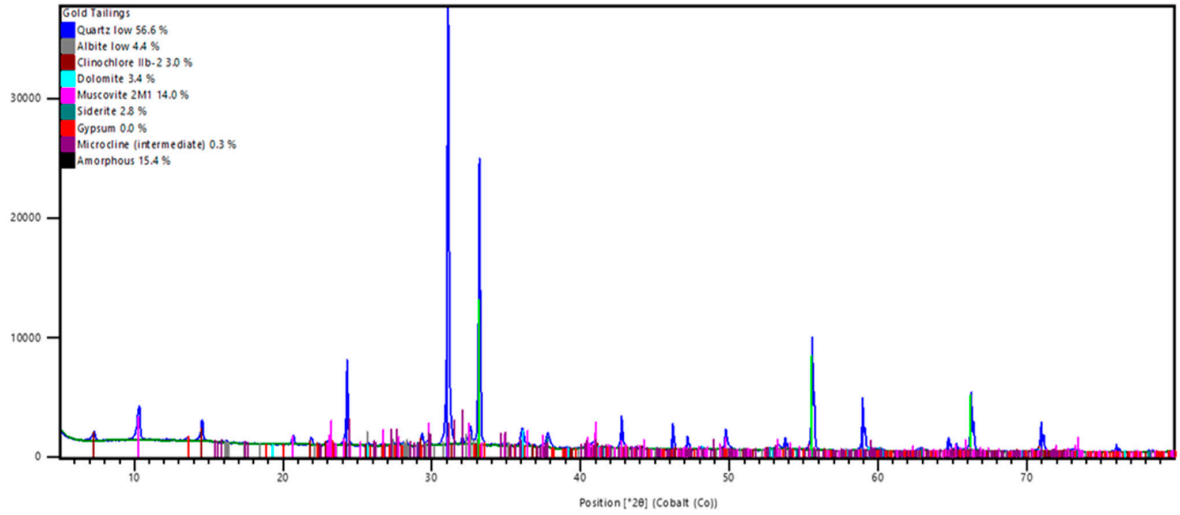


Figure 7. XRD pattern of the secondary gold tailings.

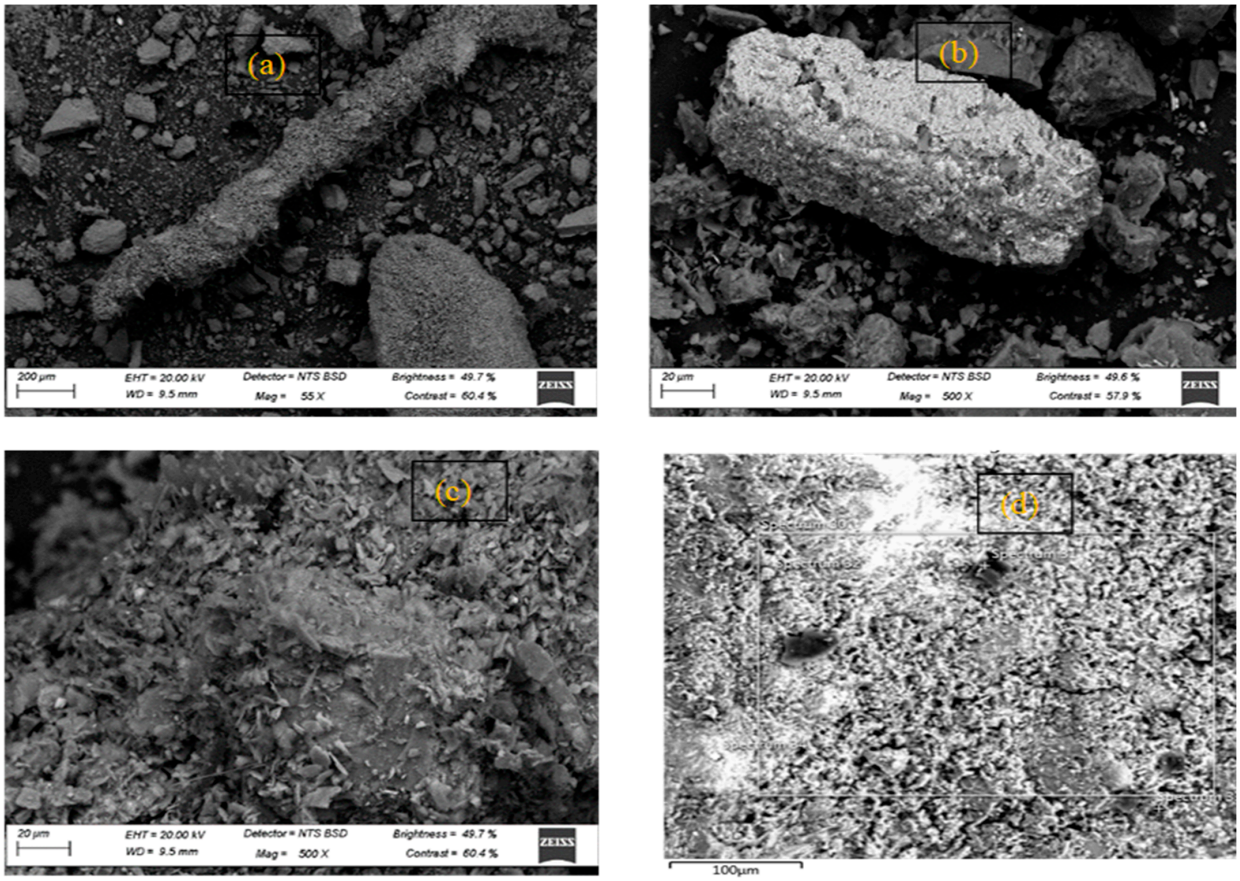


Figure 8. SEM image of (**a**–**c**) the secondary gold tailings and (**d**) the crusher sand.

Moreover, the particle size distributions of SGTs and andesite crusher sand and shown in Figure 9. The proportion of SGTs that passed through 300 µm, 150 µm, and 75 µm sieves was 86%, 66%, and 32%, while the percentage of crusher sand particles that passed through the same sieves was 20%, 12%, and 5%, respectively. This indicates that the particles of SGTs were finer than those of crusher sand. The finer the particle size, the higher is the specific surface area [52]. Therefore, SGTs have a high specific surface area compared with andesite crusher sand because of their finer particles.

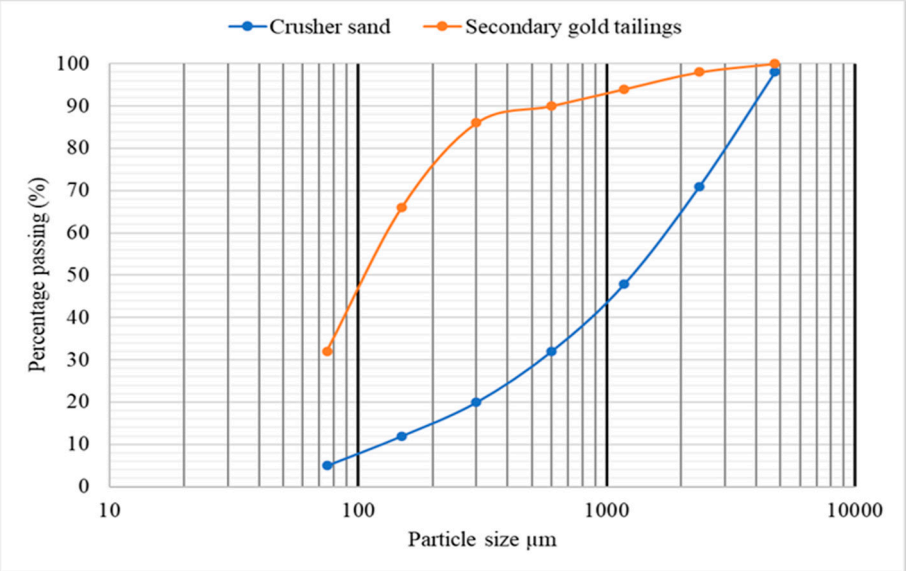


Figure 9. The particle size distribution of the secondary gold tailings and andesite crusher sand.

It was observed that SGTs had a low density compared with andesite crusher sand; their true densities were 2.76 g/cm^3 and 2.94 g/cm^3, respectively. Also, SGTs and crusher sand had bulk densities of roughly 1522 kg/cm^3 and 2011 kg/cm^3, respectively. SGTs' lower densities could be attributed to their soft mineral content, finer particles, prolonged weathering exposure, and lower iron content [30,53]. The physical properties of SGTs and andesite crusher sand are presented in Table 3.

Table 3. The physical properties of secondary gold tailings and andesite crusher sand.

Property	Secondary Gold Tailings	Andesite Crusher Sand
Fineness modulus	0.66	3.19
Density (g/cm^3)	2.76	2.94
Bulk density (kg/m^3)	1522	2011
Water absorption (%)	5.87	3.90
Shape	Angular	Angular
Surface texture	Very Rough	Rough

3.2. Workability

The workability of concrete decreased when andesite crusher sand was replaced with SGTs. As shown in Figure 10, it was observed that when the Sika ViscoCrete 3088 superplasticizer of 0.06%, 0.078%, 0.85%, 1.23%, 1.58%, and 1.96% by weight of cement was added to the mixes GT0, GT10, GT25, GT50, GT75, and GT100, respectively, the slump values increased with the increasing SP dosage in the mixtures. This was because when the SGT proportion in the mix increased compared with the preceding mixes, the mixture became stiffer and unworkable with a lower SP dosage. Consequently, when the dosage

percentage increased, the fluidity increased, making the mix workable and increasing the slump value. This might be attributed to the increase in muscovite content as the SGT proportion increased in the mixes. However, the mixes containing SGTs started to change, becoming more and more rubbery and spongy. As a result, in comparison to the reference mix, the slump values for 10%, 25%, 50%, 75%, and 100% replacement levels increased by 14%, 7%, 14%, 12%, and 18%, respectively. While the mixes gained cohesion, their increased SGT content made them stickier and consequently less manageable compared with the reference concrete. This change might have been due to the rising muscovite content with increasing SGT proportion in the concrete. Muscovite, being a clay mineral, contributes to the viscosity of the concrete mixture in its fresh state. The higher the muscovite content in the concrete, the greater is its viscosity, and subsequently, the higher the slump of the concrete [54–57].

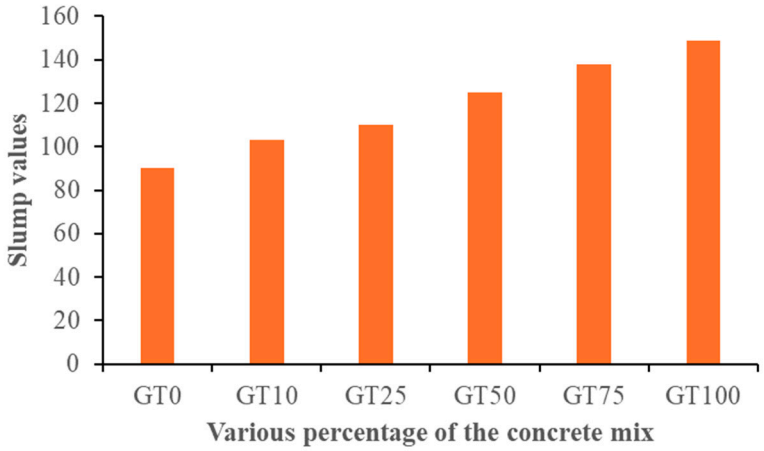


Figure 10. Slump value of concrete with and without secondary gold tailings before and after the addition of superplasticizer.

3.3. Fresh Concrete Density

Figure 11 shows the results for the fresh concrete density of the different mixes utilized in this investigation. As the SGT proportion increased up to 25%, there was a corresponding rise in fresh density. The increase can be attributed to the finer particles of SGTs equally distributed within the concrete, effectively filling the pores and consequently enhancing the compacted weight [58].

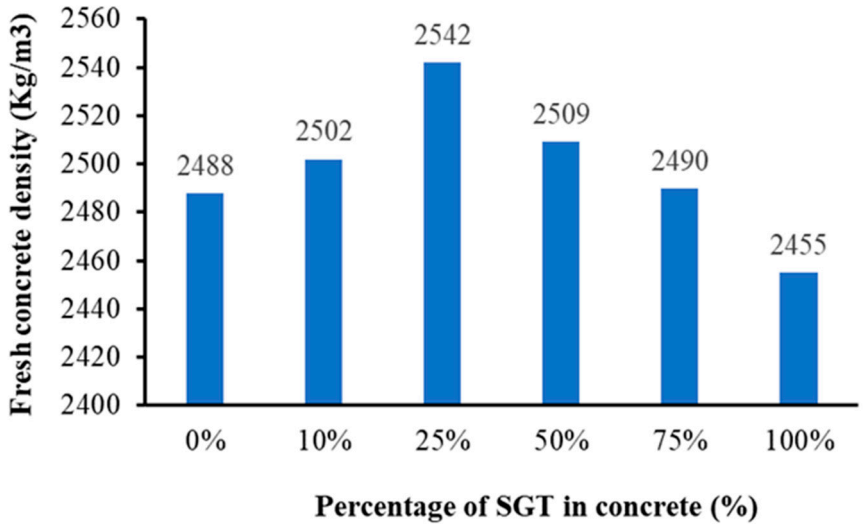


Figure 11. The fresh density of the concrete mix.

Nevertheless, beyond the 25% substitution of crusher sand with SGTs, the fresh density was reduced. This reduction might be ascribed to an excess of SGT fineness within the concrete mix, leading to the non-uniform dispersion of SGT particles throughout the mixture. As a result, the compaction decreased because some of the SGT particles might not have adhered effectively to the cement paste [59]. Additionally, every percentage replacement except for the concrete with 100% SGT replacement exhibited high fresh concrete density in comparison to the reference concrete. This could be ascribed to the filling effect of the SGT particles within the concrete. It was observed that concrete containing 100% SGT had a low density, due to the low density of SGTs compared with crusher sand [60].

3.4. Compressive Strength

Figure 12 and Table A1 in Appendix A show the results for the compressive strength of concrete with varied replacement levels of andesite crusher sand with SGT, at curing ages of 7, 28, 56, and 90 days. It was observed that the compressive strengths increased until a 25% replacement level, for all the curing periods. The compressive strength for GT10 and GT25 increased by 0.29% and 46.81% at 7 days; 0.46% and 4.01% at 28 days; 0.40% and 4.78% at 56 days; and 0.25% and 5.50% at 90 days, respectively, compared to GT0. The rise in compressive strength may have been caused by the rough surface texture and angular shape of the SGTs, which improved the bond strength between SGTs and cement paste. Additionally, the SGTs' finer particles had a filling effect on the concrete pores, which increased compaction within the concrete [61]. The results showed that for all percentage replacements, the compressive strength increased as the curing age increased. This suggested that the continuous hydration of cement within the concrete was not obstructed by the presence of SGTs in the concrete [28].

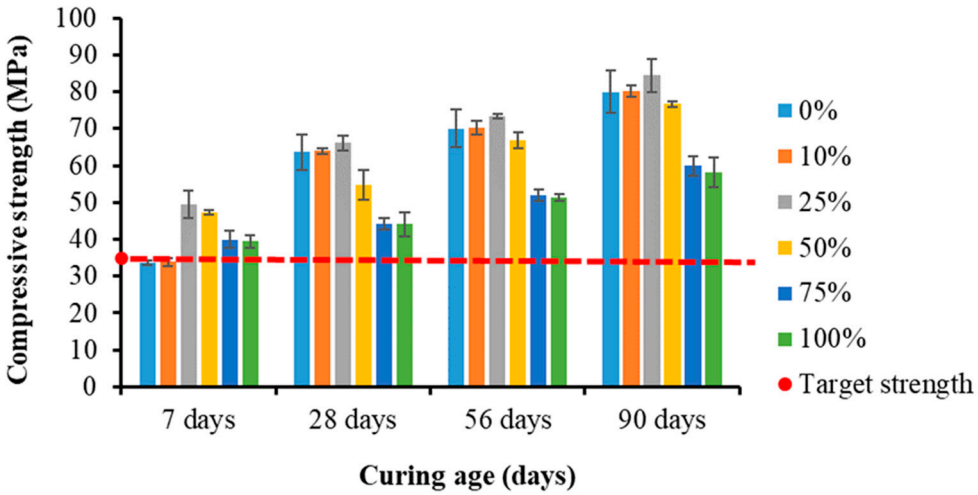


Figure 12. Compressive strength of the concrete specimens.

However, when the replacement level was above 25%, the compressive strength decreased with increased SGT proportion, for all curing periods. In comparison to GT0, the compressive strength for GT50, GT75, and GT100 decreased by 13.94%, 30.63%, and 30.74% at 28 days; 4.57%, 25.75%, and 26.72% at 56 days; and 4.10%, 25.07%, and 27.36% at 90 days, respectively. However, the decrease in compressive strength percentage for GT50 was minimal in comparison to GT75 and GT100. This suggests that while finer SGT particles had a filler effect on the GT50 pores, it was not as potent as it was for GT10 and GT25. The reduced compressive strength might have been due to the large surface area of the SGTs causing insufficient cement paste per unit area of SGT particle. This weakened the bond strength and caused agglomeration of the SGT fine particles due to electrostatic interaction, decreasing the concrete's compressive strength [52,61].

Also, the decrease in compressive strength might have been due to the higher concentration of muscovite mineral found in the SGTs, which increased as the SGT proportion in the concrete increased. The presence of muscovite particles in the concrete resulted in a smooth surface finish, causing a weaker bond between the SGTs and the cement paste [62,63]. Nevertheless, aside from the 0% and 10% replacement levels at 7 days, every concrete sample for all percentage replacement levels and curing ages achieved the target strength of 35 MPa or above.

The results followed a similar trend to the studies conducted by Preethi et al. [29] and Song et al. [32], where compressive strengths increased to a certain level of replacement before decreasing. Specifically, Preethi et al. [29] recorded the highest compressive strength at 15% replacement of river sand with gold tailings at 3, 7, and 28 days. In contrast, Song et al. [32], reported that at 28 days, the highest compressive strength was obtained at 30% replacement of river sand with gold tailings.

Statistical Analysis

The statistical analysis results for the compressive strength data are presented in Table 4 and Figures 13–17. The analysis was performed using SPSS version 26 and a regression model was established to perform the ANOVA between the concrete samples with and without SGT. The model assesses the linear relationship between a single predictor and a continuous response. In this study, the reference concrete GT0 was considered the response variable, while the different proportions of SGTs replacing crusher sand served as the predictor variables. The model applied hypothesis testing, assessing the null hypothesis by accepting or rejecting it with a measured risk level of $p \leq 0.05$ at a 95% confidence level. In this context, p signifies the probability of evaluating the compressive strength in relation to whether the null hypothesis holds. According to the null hypothesis, there is no significant distinction between the compressive strengths of concrete with and without SGTs. This suggests that SGTs have no significant effect on concrete's compressive strength.

Table 4. Result of ANOVA for the compressive strength.

Source	DF	MS	F Value	*p* Value Prob > F	Adj. R Square	Significance
GT10	1	3632.890	332.532	0.000	96.8	Yes
GT25	1	3390.316	96.364	0.000	89.7	Yes
GT50	1	2714.851	26.427	0.000	69.8	Yes
GT75	1	2672.334	24.980	0.001	68.6	Yes
GT100	1	2352.070	16.921	0.002	59.1	Yes

Based on the ANOVA results, the chosen model accurately portrayed the collected data. Across all models, the p values were below 0.05, indicating that each model term held statistical significance at a 95% confidence level. Moreover, the model confidence levels surpassed 95%, confirming their robustness. The correlation coefficient, R^2, indicated that the established models explained between 59.1% to 96.8% of the variations in compressive strengths, indicating a satisfactory fit with the data. This showed a good correlation coefficient between the compressive strength of the reference concrete and different mixes, suggesting that SGTs had a significant impact on the concrete's compressive strength.

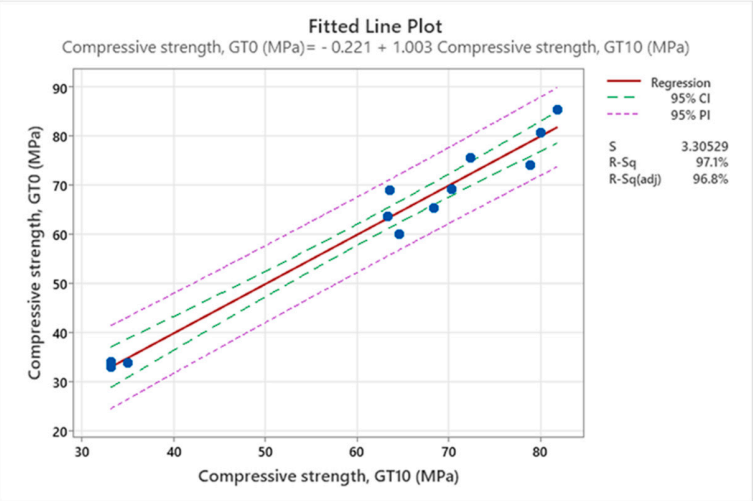


Figure 13. Fitted line plot showing regression analysis of compressive strength, for reference concrete against concrete made with 10% SGT.

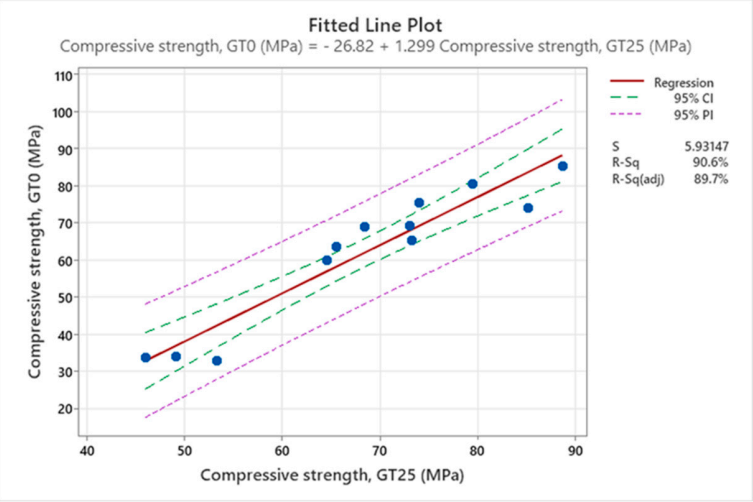


Figure 14. Fitted line plot showing regression analysis of compressive strength, for reference concrete against concrete made with 25% SGT.

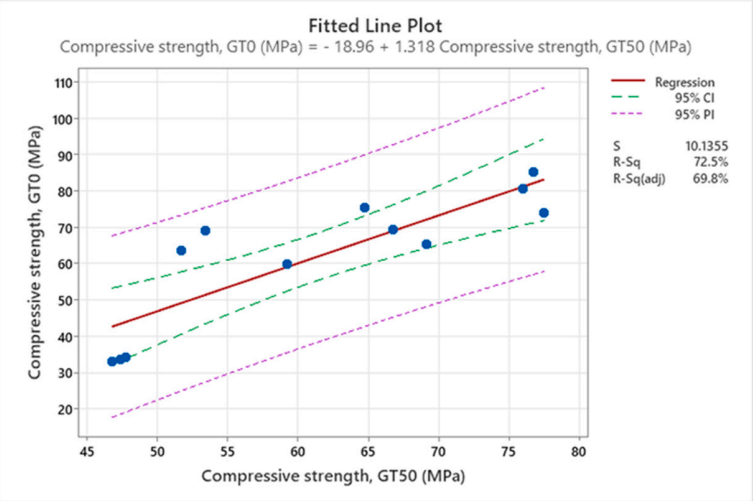


Figure 15. Fitted line plot showing regression analysis of compressive strength, for reference concrete against concrete made with 50% SGT.

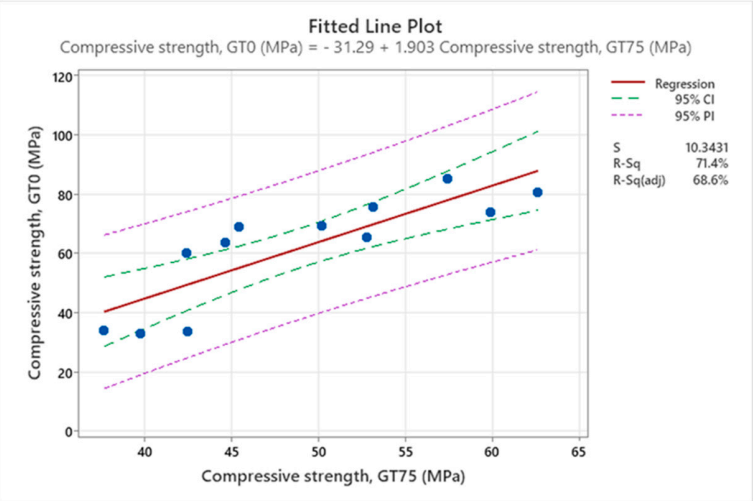


Figure 16. Fitted line plot showing regression analysis of compressive strength, for reference concrete against concrete made with 75% SGT.

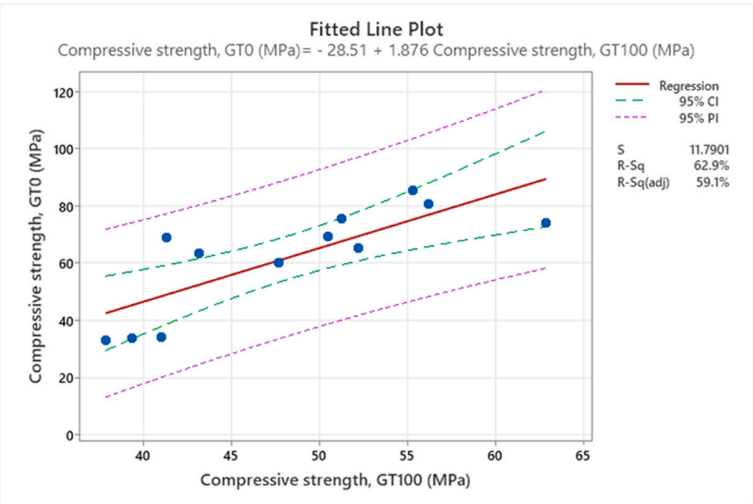


Figure 17. Fitted line plot showing regression analysis of compressive strength, for reference concrete against concrete made with 100% SGT.

3.5. Splitting Tensile Strength

Figure 18 and Table A2 in Appendix A show the splitting tensile strength results for concrete with different proportions of andesite crusher sand replaced with SGTs, after curing periods of 7, 28, 56, and 90 days. It was observed that for each curing age, the compressive strengths increased up to a 50% substitution of crusher sand with SGTs. For GT10, GT25, and GT50, the increased percentages of splitting tensile strengths in comparison to GT0 were as follows: 17.32%, 40.69%, and 44.16% after 7 days; 2.17%, 2.80%, and 33.23% after 28 days; 1.34%, 3.79%, and 5.36% after 56 days; and 0.41%, 3.04%, and 11.13% after 90 days, respectively. The higher splitting tensile strength might have been caused by the filling effect of very fine SGT particles enhancing adhesion between aggregates and cement paste [64]. Also, the angular shape and rough surface texture of SGTs contributed to the higher splitting tensile strength by improving interlocking among aggregates in the concrete mix, thereby increasing bond strength [52]. It was noticed that for all percentage replacement levels, concrete splitting tensile strength increased with increased curing ages, indicating that the incorporation of SGTs did not impede the continuous hydration of cement within the concrete [28].

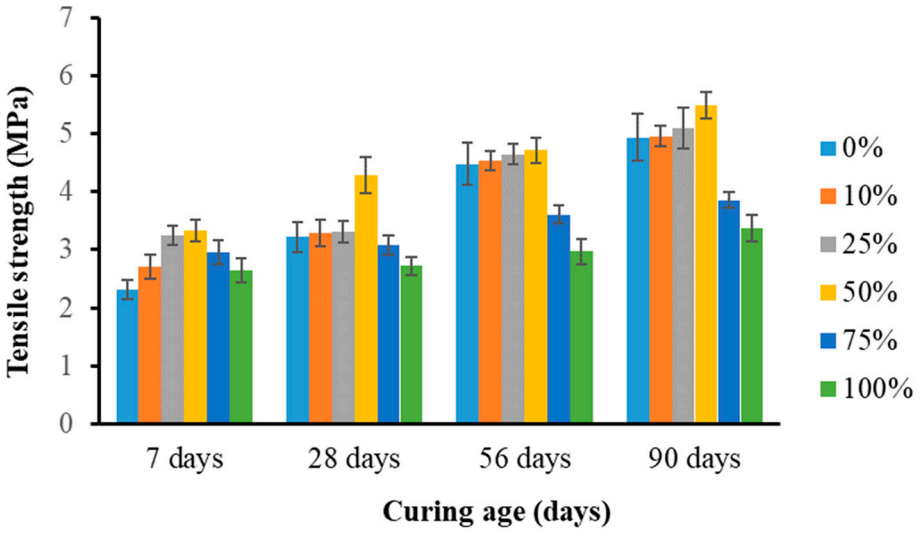


Figure 18. Splitting tensile strength of the concrete specimens.

However, as the replacement level exceeded 50%, there was a decline in the splitting tensile strength. Additionally, concrete with replacement levels of 75% and 100% exhibited low splitting tensile strength compared with the reference concrete after curing periods of 28 days, 56 days, and 96 days. The splitting tensile strength for GT75 and GT100 relative to GT0 was observed to decrease by the following percentages: 4.35% and 15.53% at 28 days; 19.42% and 33.71% at 56 days; 21.86% and 31.78% at 90 days, respectively. The presence of soft minerals like muscovite in SGTs might have been the cause of the decreased splitting tensile strength. The proportion of soft minerals in the concrete increased as the proportion of SGTs increased, resulting in the formation of a weak bond between the SGT particles and the cement matrix. As a result, the splitting tensile strength decreased [30].

Comparable trends were observed in the findings of the study by Song et al. [28], which found that splitting tensile strengths rose up to a specific replacement level before declining. They recorded the highest splitting tensile strengths at 30% replacement of river sand with gold tailings.

3.6. The Relationship between Splitting Tensile Strength and Compressive Strength

Results for compressive strength and splitting tensile strength showed that the splitting tensile strength of the concrete specimens varied along a similar pattern to the compressive strength. This trend was similar to previous report [28], stating that the incorporation of gold tailings produced higher compressive and splitting tensile strengths than reference concrete, up to a certain replacement level. However, the strengths decreased as the percentage of gold tailings in the concrete increased. In this study, contrary to the compressive strength, it was obvious that substituting 50% of the crusher sand with SGTs gave the maximum splitting tensile strength, for all curing ages. The correlation coefficients were determined, in order to establish the relationship between splitting tensile strength and compressive strength.

Figure 19 shows the results of the relationship, including the linear equation that describes the relationship. Within the equations, the variable y″ represents splitting tensile strength, while x″ stands for compressive strength. The correlation coefficients were determined to be 0.88, 0.82, 0.78, 0.95, 0.98, and 0.95 for 0%, 10%, 25%, 50%, 75%, and 100%, respectively. This suggests that splitting tensile strength and compressive strength have a good relationship. Even though scatter was observed in the results, at specific replacement levels, splitting tensile strength increased as compressive strength increased and diminished as compressive strength decreased.

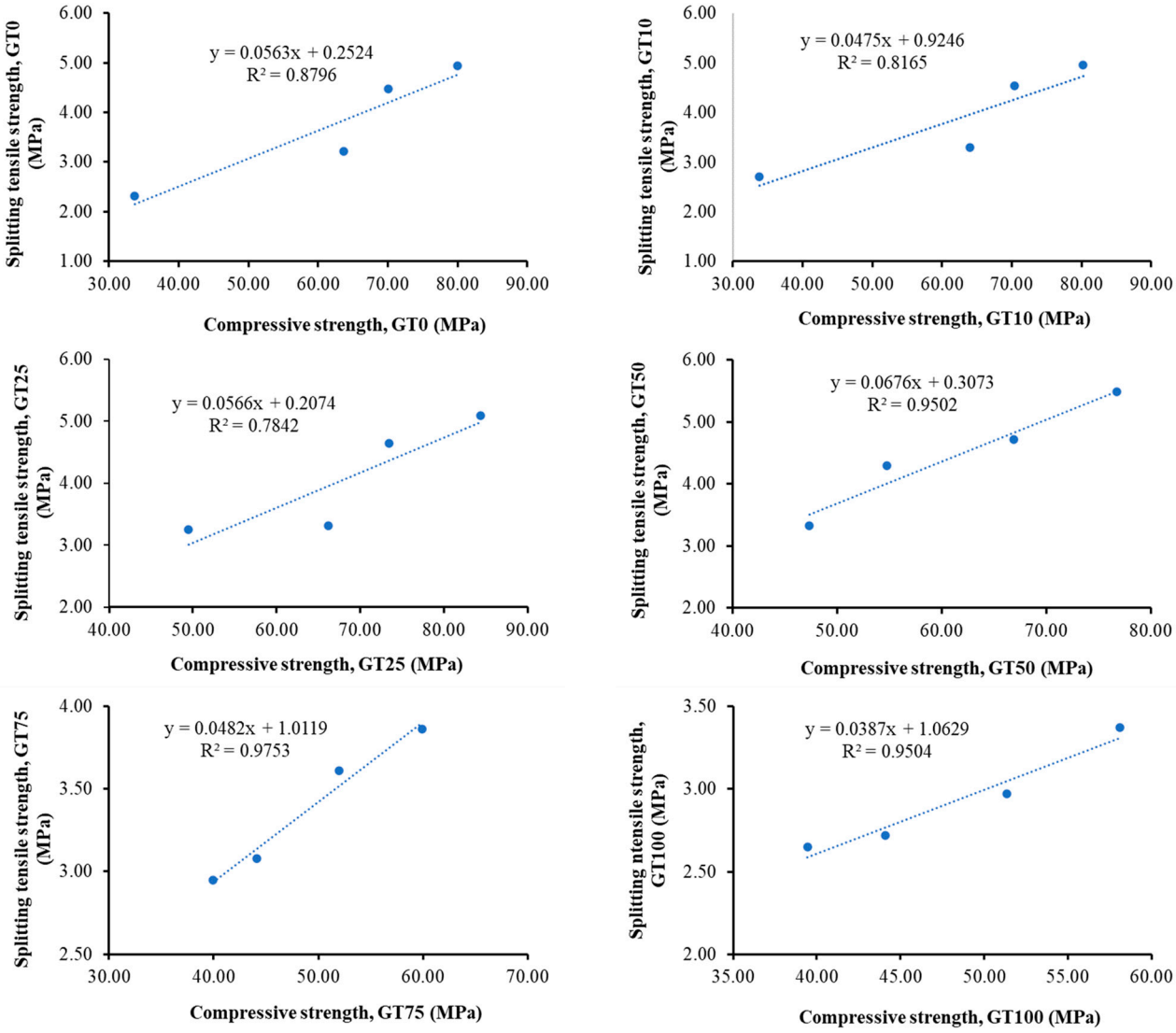


Figure 19. Relationship between splitting tensile strength and compressive strength.

3.7. Durability Properties

Durability properties were evaluated using durability indices such as oxygen permeability, water sorptivity, and chloride conductivity indices. These also served the purpose of analyzing the porosity of the concrete. The durability indices were evaluated based on the average values derived from four concrete specimens, for curing periods of 28, 56, and 90 days. The grading ranges according to the South African Standard were used to assess the quality of the concrete [65].

3.7.1. Oxygen Permeability

Figure 20 and Table A3 in Appendix A show the oxygen permeability index (OPI) results for each percentage replacement level after 28, 56, and 90 days of curing. It is important to note that the permeability of the concrete reduced as the OPI value increased. It was observed that as the curing periods increased, the OPI value increased. The optimum OPI after 28, 56, and 90 days was achieved at 100%, 0%, and 50% replacement levels, respectively. After 90 days of curing, the average OPI values for both 25% and 50% replacement levels were more than that of the reference concrete. This might have been due to the SGTs' filler effect, which aided in refining the pores [66].

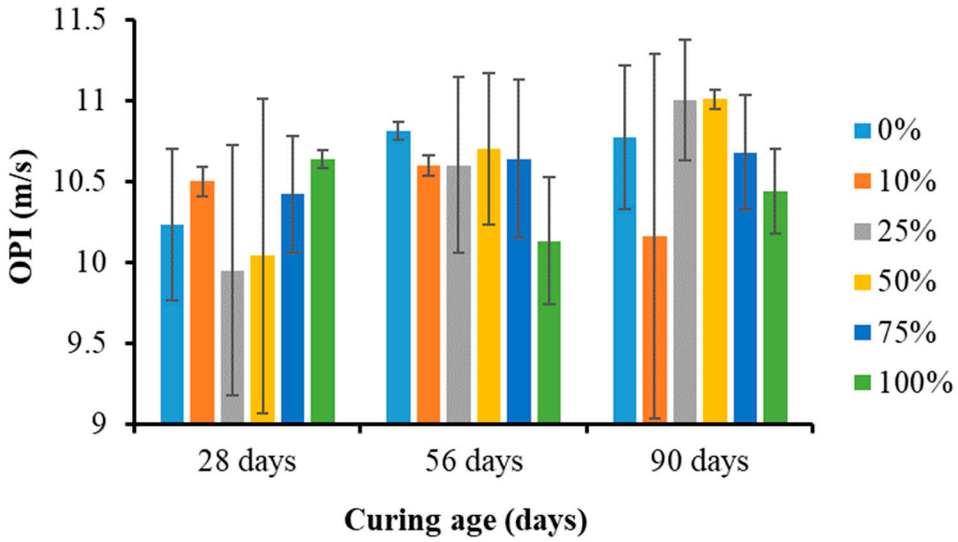


Figure 20. Oxygen permeability indices of concrete specimens.

The OPI results ranged from 9.95 to 11.01, classified as good concrete quality for values between 9.5–10 and excellent concrete quality for values greater than 10, according to South African Standard [65]. The OPI values of the concrete specimens after all curing periods were within the range for excellent concrete quality according to the South African Standard, except for the GT25 OPI value after 28 days, which was within the range for good concrete quality. This signified that regardless of the replacement level percentage, concrete containing SGTs had good resistance to oxygen permeability. The slight differences among the OPI values of the concrete samples indicated that the test might be less sensitive to changes in SGT proportions. Also, the large deviation in the error bar might be due to the large variability within the results of the same sets of samples, which might have been caused by the rate at which oxygen penetrated each sample [67]. The oxygen permeability of concrete containing gold tailings has yet to be reported in the literature. However, the current oxygen permeability results are consistent with the research conducted by Thomas et al. [60], where concrete containing copper tailings as replacement for river sand was less susceptible to air permeability.

3.7.2. Water Sorptivity

The results of the water sorptivity index (WSI) for each percentage replacement level after curing periods of 28, 56, and 90 days are shown in Figure 21 and Table A4 in Appendix A. The concrete's WSI values signify the rate at which water passes through concrete via capillary suction, normalized by porosity; the lower the WSI value, the higher the resistance of the concrete to moisture penetration. It was observed that for all curing ages, the WSI values of GT25, GT50, GT75, and GT100 remained lower than those of the reference concrete (GT0). This might have been caused by the SGT particles' filler action, which improved the concrete's pore structure [68]. Contrarily, GT10 had high WSI values compared with GT0. This might be attributed to the non-uniform distribution of SGT particles within the concrete, exerting minimal influence on interrupting capillary formation and consequently causing a higher capillary absorption rate [69]. The WSI results ranged from 5.79–9.69, categorized as good concrete quality for values between 6–10 and excellent concrete quality for values less than 6, as per South African Standards [65]. This indicated that concretes made with SGTs were not vulnerable to water penetration. Although the water sorptivity of concrete containing gold tailings has not been documented in the literature, the results are similar to the water absorption findings in the study conducted by Song et al. [32], and Ahmed et al. [30], indicating that concrete containing gold tailings has lower water absorption.

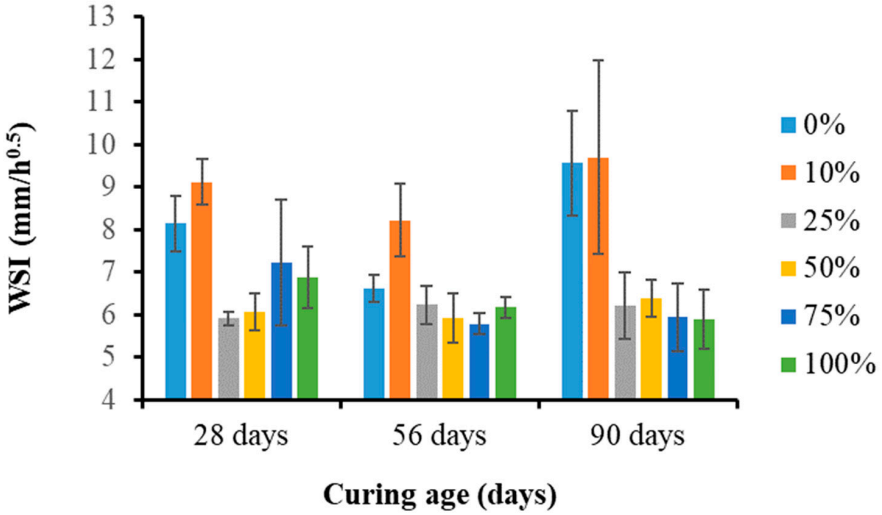


Figure 21. Water sorptivity indices of concrete specimens.

3.7.3. Chloride Conductivity

Figure 22 and Table A5 in Appendix A present the chloride conductivity index (CCI) results for various percentage replacement levels after 28, 56, and 90 days of curing. It is crucial to understand that when the CCI value increased, the concrete's chloride conductivity increased. It was observed that the CCI value decreased with increasing curing ages. Also, in comparison to reference concrete, the CCI of GT10, GT75, and GT100 was higher after 90 days of curing, while it was lower for GT25 and GT50. The increased CCI in the concrete containing SGTs might have been due to the higher specific surface area of the SGTs, resulting in inadequate cement paste coverage on each SGT particle's unit area. This led to a decrease in aggregate adhesion, subsequently reducing the resistance to chloride penetration [70]. However, the filler effect of SGTs might be the reason for the reduced CCI in some concrete containing SGTs. This greatly improved the concretes' resistance to chloride penetration and reduced the pore size. The CCI values ranged from 0.13 to 3.24 and at 90 days, in accordance with South African Standards, all of the concrete samples were found to be of good quality and excellent quality for values between 0.75–1.5 and values less than 0.75, respectively [65]. Apart from chloride permeability, the literature has not addressed the chloride conductivity of concrete containing gold tailings. In contrast to chloride conductivity findings, Song et al. [32] found that concrete with higher proportions of gold tailings had lower chloride ion permeability compared with concrete with a lower proportion of gold tailings or reference concrete.

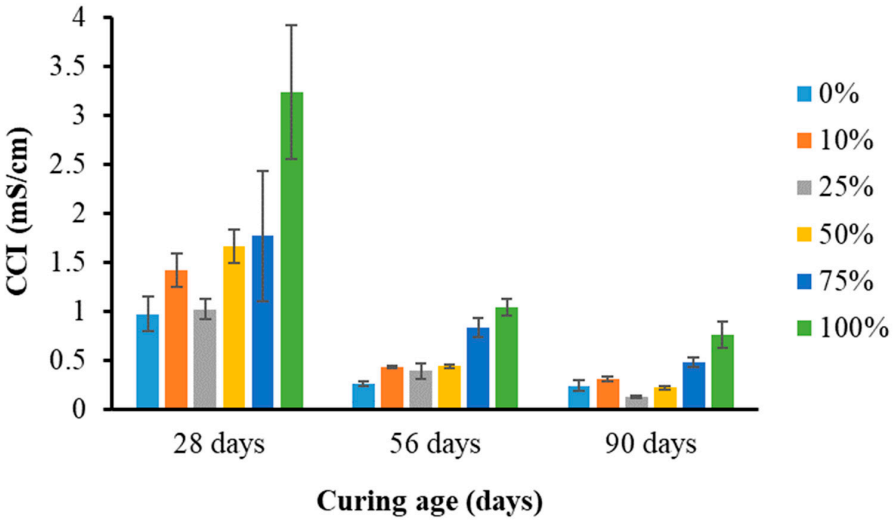


Figure 22. Chloride conductivity indices of concrete specimens.

3.7.4. Porosity

The porosity results for the concrete specimens with various percentage replacement levels that were soaked with calcium hydroxide after 28, 56, and 90 days of curing are shown in Figure 23 and Table A6 in Appendix A. It was observed that for every percentage replacement level, the porosity reduced with increasing curing age. The decrease in concrete porosity at 56 and 90 days, compared with 28 days, was as follows: 20.36% and 28.33% for GT0; 14.70% and 24.23% for GT10; 14.34% and 51.07% for GT25; 8.50% and 32.03% for GT50; 7.60% and 20.91% for GT75; and 8.20% and 24.86% for GT100, respectively. This indicates that when SGTs were used in place of crusher sand in concrete, the chemical composition did not hinder the primary hydration of cement. Additionally, it suggests an enhancement in the pore structures. Furthermore, among all percentage replacement levels, 25% replacement level produced the lowest porosity throughout the curing ages. This could be attributed to the filler effect in which the very fine particles of SGTs were evenly distributed and filled up the concrete's pores [66,71].

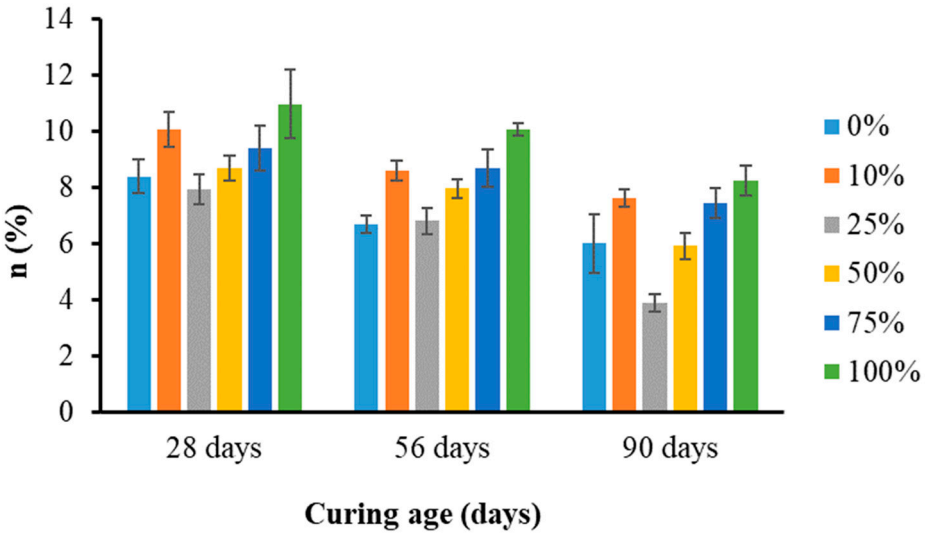


Figure 23. Porosity of concrete specimens saturated with calcium hydroxide.

Furthermore, Figure 24 and Table A7 in Appendix A show the porosity of concrete specimens that were saturated with a sodium chloride solution. It was observed that the porosity of the concrete specimens over curing periods from 28 to 90 days followed a similar trend to those observed in concretes saturated with calcium hydroxide solution. Nevertheless, compared to the concretes saturated with calcium hydroxide solution, the porosity after curing for 28, 56, or 90 days was 46.19% to 62.36% lower. Variations in the density of the two solutions were responsible for the observed pattern of reduced porosity in the concrete treated with sodium chloride [45,67]. The robustness of the porosity results is indicated by the similarity in the porosity patterns for the two saturating solutions. In comparison to the results of the current study, Song et al. [32] observed that concrete with 30% gold tailings showed the highest reduction in porosity. Beyond the 30% replacement level, the porosity increased but was lower than that observed at the 20% replacement level.

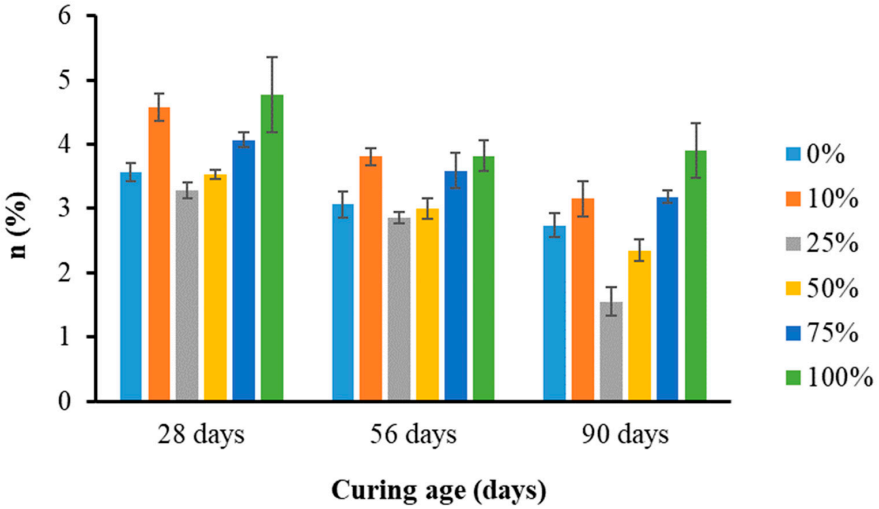


Figure 24. Porosity of the concrete specimens saturated with sodium chloride.

4. Applications

This investigation demonstrates the viability of using SGTs as a substitute for crusher sand in producing sustainable concrete. Concrete serves as the backbone of structures. Thus, concrete made with SGTs can be applied to different parts of a structure. The various parts of the structure include the substructure (foundation and basement), superstructure (lintels, stairways, walls, and roof), and other structural elements (slabs, columns, beams, and floor). The practical use of concrete containing SGTs offers a way to lessen the substantial quantity of stockpiled SGTs. Additionally, it decreases the massive amount of crusher sand needed for concrete production, conserving natural resources. Consequently, this can reduce the overall cost of concrete production in mining environments. The mining and concrete industries can collaborate based on the practical application of concrete containing SGT. The collaboration proves advantageous for both sectors, as it diminishes the expenses associated with crusher sand in concrete production and reduces the volume of tailings that need to be handled. Overall, this promotes sustainable development in the mining and concrete industries, and the environment.

5. Conclusions and Recommendations

This study investigated the feasibility of replacing conventional sand with SGT to produce sustainable concrete. Various proportions of SGTs (0%, 10%, 25%, 50%, 75%, and 100%) were used in producing sustainable concrete. According to the results and discussion outlined in the previous section, the following conclusions are drawn:

1. SGTs are reprocessed gold tailings from which some metals have been recovered, and they are considered relatively inert due to the absence of sulfide and pyrite, making them environmentally friendly. They contain soft minerals and a high muscovite content that could influence the properties of concrete. SGTs have finer particles, low densities, high specific surface area, and high water absorption compared with andesite crusher sand. However, the similarity in the properties of SGTs and andesite crusher sand makes SGTs a potential material for andesite crusher sand substitution in concrete production.
2. The inclusion of SGTs as fine aggregate decreased the workability due to finer particles, high specific surface area, and high water absorption of the SGTs. The workability of concrete containing SGTs can be improved by adding superplasticizers, regardless of SGT content in the concrete mix. The replacement of andesite crusher sand with SGTs up to 75% enhanced the density of concrete compared with andesite crusher sand, while the highest density was obtained at a 25% replacement level.
3. The compressive strength of concrete with up to 25% replacement of crusher sand with SGTs is high compared with the reference concrete, for all curing ages. Beyond the 25% replacement level, the compressive strength was lower than that of the reference concrete for all curing ages. However, all the concrete samples at 28, 56, and 90 days

met the target strength. The highest compressive strength was obtained at a 25% replacement level. The ANOVA analysis results validated that the percentage of SGT significantly impacted the compressive strength of concrete for curing periods of 7, 28, 56, and 90 days. The splitting tensile strength of the concretes followed a similar trend to that of compressive strength. However, the splitting tensile strength increased up to 50% for all curing ages but then decreased. The highest splitting tensile strength was achieved at a 50% replacement level. This indicates that SGTs can partially replace crusher sand and produce concrete with desirable mechanical properties.

4. Concrete made with SGTs as a replacement for crusher sand had similar OPI and WSI to reference concrete. The concrete samples' OPI ranged from 9.95 to 11.01 and WSI ranged from 5.79–9.69, placing them within the good to excellent category for concrete quality in terms of OPI and WSI, respectively. Concrete made with SGTs showed strong resistance to oxygen permeability and water sorptivity, irrespective of the percentage replacement levels, for all curing ages. Also, after 56 and 90 days, the CCI of concretes with and without SGTs was found to reflect good to excellent concrete quality, indicating good resistance to chloride penetration. Concrete samples also showed a reduction in porosity with increasing curing periods. This indicates that concrete containing SGTs as a substitute for crusher sand is durable.
5. This study demonstrates that like primary gold tailings, SGTs can be used as fine aggregate in concrete production, indicating that the substitution potential of gold tailings is not limited to river sand. The results of this study suggest that SGT is environmentally friendly and can be efficiently substituted for crusher sand in concrete. In addition to its strength performance, this study further shows the satisfactory durability performance of concrete containing gold tailings. Using SGTs as fine aggregate in concrete can reduce the space occupied by tailings disposal, conserve natural resources, and lessen environmental problems. It also reduces the use of conventional fine aggregate and lowers the cost compared with using conventional fine aggregate for concrete production, particularly in mining environments. Additionally, it would represent a reduction in carbon emissions associated with conventional fine aggregate (crusher sand) production, as SGTs require no additional processing to achieve the necessary particle size. This study can offer direction for conducting a more comprehensive investigation into utilizing secondary gold tailings in concrete.
6. It is necessary to investigate other important properties such as resistance to sulfate attack, carbonation depth, alkali–silica reaction, drying shrinkage, microstructural behavior, corrosion, and thermal properties to understand the performance of the concrete from these aspects.
7. Due to the satisfactory performance of concrete containing SGTs, it can be effectively employed as a construction material. This utilization of SGTs helps address sand sustainability concerns in producing sustainable concrete, promoting a greener environment.

Author Contributions: Conceptualization, J.O.I.; writing—original draft preparation; R.A.A.; writing—reviewing and editing; J.O.I., M.O. and R.A.A.; supervision; J.O.I. and M.O.; visualization; M.O., J.O.I. and R.A.A.; project administration: J.O.I. and M.O. All authors have read and agreed to the published version of the manuscript.

Funding: This research was funded by the Durban University of Technology South Africa Research Scholarship and Future Professor program [GOOT-02S8GT019]. The APC was funded by the University of the Watersrand, Johannesburg, South Africa.

Institutional Review Board Statement: Not applicable.

Informed Consent Statement: Not applicable.

Data Availability Statement: The data is strictly belong to the Durban University of Technology, South Africa.

Acknowledgments: The Durban University of Technology, Pietermaritzburg, South Africa is acknowledged for their financial support. The University of the Witwatersrand, Johannesburg South Africa is acknowledged for the use of their laboratory to conduct the experiment reported in this study.

Conflicts of Interest: The authors declare no conflicts of interest.

Appendix A

Table A1. Compressive strength of concrete specimens.

Mixes	Compressive Strength (MPa)			
	7 Days	28 Days	56 Days	90 Days
0%	33.71	63.64	70.05	80.01
10%	33.81	63.93	70.33	80.21
25%	49.49	66.19	73.40	84.21
50%	47.33	54.77	66.85	76.73
75%	39.96	44.15	52.01	59.59
100%	39.43	44.08	51.33	58.12

Table A2. Splitting tensile strength of concrete specimens.

Mixes	Splitting Tensile Strength (MPa)			
	7 Days	28 Days	56 Days	90 Days
0%	2.31	3.22	4.48	4.94
10%	2.71	3.29	4.54	4.96
25%	3.25	3.31	4.65	5.09
50%	3.33	4.29	4.72	5.49
75%	2.95	3.08	3.61	3.86
100%	2.65	2.72	2.97	3.37

Table A3. Oxygen permeability index of concrete specimens.

Mixes	Oxygen Permeability Index		
	28 Days	56 Days	90 Days
0%	10. 23	10.81	10.77
10%	10.50	10.60	10.16
25%	9.95	10.60	11.00
50%	10.04	10.70	11.01
75%	10.42	10.64	10.68
100%	10.64	10.13	10.44

Table A4. Water sorptivity index of concrete specimens.

Mixes	Water Sorptivity Index		
	28 Days	56 Days	90 Days
0%	8.14	6.68	9.57
10%	9.12	8.22	9.69
25%	5.91	6.23	6.21
50%	6.07	5.92	6.39
75%	7.23	5.79	5.94
100%	6.88	6.17	5.89

Table A5. Chloride conductivity index of concrete specimens.

Mixes	Chloride Conductivity Index		
	28 Days	56 Days	90 Days
0%	0.97	0.26	0.24
10%	1.42	0.43	0.31
25%	1.02	0.39	0.13
50%	1.66	0.44	0.22
75%	1.77	0.83	0.48
100%	3.24	1.04	0.76

Table A6. Porosity of concrete specimens saturated with calcium hydroxide.

Mixes	Porosity with Calcium Hydroxide		
	28 Days	56 Days	90 Days
0%	8.40	6.69	6.02
10%	10.07	8.59	7.63
25%	7.95	6.81	3.89
50%	8.71	7.97	5.92
75%	9.42	8.7	7.45
100%	10.98	10.08	8.25

Table A7. Porosity of concrete specimens saturated with sodium hydroxide.

Mixes	Porosity with Sodium Hydroxide		
	28 Days	56 Days	90 Days
0%	3.56	3.06	2.74
10%	4.58	3.81	3.15
25%	3.28	2.85	1.55
50%	3.53	3.00	2.35
75%	4.07	3.59	3.18
100%	4.77	3.82	3.90

References

1. Ahmad, J.; Majdi, A.; Babeker Elhag, A.; Deifalla, A.F.; Soomro, M.; Isleem, H.F.; Qaidi, S. A Step towards Sustainable Concrete with Substitution of Plastic Waste in Concrete: Overview on Mechanical, Durability and Microstructure Analysis. *Crystals* **2022**, *12*, 944. [CrossRef]
2. Tangaramvong, S.; Nuaklong, P.; Khine, M.T.; Jongvivatsakul, P. The influences of granite industry waste on concrete properties with different strength grades. *Case Stud. Constr. Mater.* **2021**, *15*, e00669. [CrossRef]
3. Sankh, A.C.; Biradar, P.M.; Naghathan, S.J.; Ishwargol, M.B. Recent Trends in Replacement of Natural Sand with Different Alternatives. *IOSR J. Mech. Civ. Eng.* **2018**, 59–66. Available online: www.iosrjournals.org (accessed on 2 September 2024).
4. Khouadjia, M.L.K.; Mezghiche, B.; Drissi, M. Experimental evaluation of workability and compressive strength of concrete with several local sand and mineral additions. *Constr. Build. Mater.* **2015**, *98*, 194–203. [CrossRef]
5. Ahmad, J.; Zhou, Z.; Martínez-García, R.; Vatin, N.I.; De-Prado-gil, J.; El-Shorbagy, M.A. Waste Foundry Sand in Concrete Production Instead of Natural River Sand: A Review. *Materials* **2022**, *15*, 2365. [CrossRef] [PubMed]
6. Stempkowska, A.; Gawenda, T.; Naziemiec, Z.; Adam Ostrowski, K.; Saramak, D.; Surowiak, A. Impact of the geometrical parameters of dolomite coarse aggregate on the thermal and mechanic properties of preplaced aggregate concrete. *Materials* **2020**, *13*, 4358. [CrossRef] [PubMed]
7. Nardelli, A.; Cacciari, P.P.; Futai, M.M. Sand–concrete interface response: The role of surface texture and confinement conditions. *Soils Found.* **2019**, *59*, 1675–1694. [CrossRef]

8. Gondo, T.; Mathada, H.; Amponsah-Dacosta, F. Regulatory and policy implications of sand mining along shallow waters of Nzhelele River in South Africa. *Jamba J. Disaster Risk Stud.* **2019**, *11*, 1–12. [CrossRef]
9. Muigai, R.; Alexander, M.G.; Moyo, P. Cradle-to-gate environmental impacts of the concrete industry in South Africa. *J. S. Afr. Inst. Civ. Eng.* **2014**, *56*, 108.
10. Lee, C. *How Can Environmental Impacts Be Evaluated in Aggregate Production*; University of Gothenburg: Gothenburg, Sweden, 2021. Available online: https://cms.it.gu.se/infoglueDeliverWorking/digitalAssets/1792/1792496_lee-c.pdf (accessed on 25 July 2024).
11. Siddique, R.; Singh, M.; Mehta, S.; Belarbi, R. Utilization of treated saw dust in concrete as partial replacement of natural sand. *J. Clean. Prod.* **2020**, *261*, 121226. [CrossRef]
12. Althoey, F.; Hosen, M.A. Physical and mechanical characteristics of sustainable concrete comprising industrial waste materials as a replacement of conventional aggregate. *Sustainability* **2021**, *13*, 4306. [CrossRef]
13. Sunarsih, E.S.; Patanti, G.W.; Agustin, R.S.; Rahmawati, K. Utilization of Waste Glass and Fly Ash as a Replacement of Material Concrete. *IOP Conf. Ser. Earth Environ. Sci.* **2021**, *1808*, 012004. [CrossRef]
14. Thiruvenkitam, M.; Pandian, S.; Santra, M.; Subramanian, D. Use of waste foundry sand as a partial replacement to produce green concrete: Mechanical properties, durability attributes and its economical assessment. *Environ. Technol. Innov.* **2020**, *19*, 101022. [CrossRef]
15. Ogola, J.; Shavhani, T.; Mundalamo, R. Possibilities of Reprocessing Tailings Dams for Gold and other Minerals: A Case Study of South Africa. *J. Environ. Sci. Allied Res.* **2018**, *2017*, 39–42. [CrossRef]
16. Weiersbye, I.M.; Witkowski, E.T.F.; Reichardt, M. Floristic composition of gold and uranium tailings dams, and adjacent polluted areas, on South Africa's deep-level mines. *Bothalia* **2006**, *36*, 101–127. [CrossRef]
17. Aderinto, G.E.; Ikotun, J.O.; Madirisha, M.M.; Katte, V. Geopolymer Cement in Pavement Applications: Bridging Sustainability and Performance, an In-Depth Review. 2024; pp. 1–30. Available online: https://www.mdpi.com/2071-1050/16/13/5417 (accessed on 2 September 2024).
18. Ikotun, J.O.; Aderinto, G.; Katte, V. Geo-polymerization of mining tailing for use as a pavement construction material: A review. In *Young Concrete Researchers, Engineers & Technologist Symposium (YCRETS)*; Cement & Concrete SA: Midrand, South Africa, 2023.
19. Chen, B.; Pang, L.; Zhou, Z.; Chang, Q.; Fu, P. Study on the activation mechanism and hydration properties of gold tailings activated by mechanical-chemical-thermal coupling. *J. Build. Eng.* **2022**, *48*, 104014. [CrossRef]
20. Gou, M.; Zhou, L.; Then, N.W.Y. Utilization of tailings in cement and concrete: A review. *Sci. Eng. Compos. Mater.* **2019**, *26*, 449–464. [CrossRef]
21. Li, S.; Chen, J.; Gao, W.; Lyu, X.; Liang, Z.; Zhou, W. Current situation and prospects for the clean utilization of gold tailings. *Waste Manag.* **2024**, *180*, 149–161. [CrossRef]
22. Mashifana, T.; Sithole, T. Clean production of sustainable backfill material from waste gold tailings and slag. *J. Clean. Prod.* **2021**, *308*, 127357. [CrossRef]
23. Wang, L.; Ji, B.; Hu, Y.; Liu, R.; Sun, W. A review on in situ phytoremediation of mine tailings. *Chemosphere* **2017**, *184*, 594–600. [CrossRef]
24. Sigvardsen, N.M.; Nielsen, M.R.; Potier, C.; Ottosen, L.M.; Jensen, P.E. Utilization of Mine Tailings as Partial Cement Replacement. *Mod. Environ. Sci. Eng.* **2018**, *4*, 365–373.
25. Wu, A.; Wang, Y.; Ruan, Z.; Xiao, B.; Wang, J.; Wang, L. Key theory and technology of cemented paste backfill for green mining of metal mines. *Green Smart Min. Eng.* **2024**, *1*, 27–39. [CrossRef]
26. Yang, L.; Jia, H.; Wu, A.; Jiao, H.; Chen, X.; Kou, Y.; Dong, M. Particle aggregation and breakage kinetics in cemented paste backfill. *Int. J. Miner. Metall. Mater.* **2024**, *31*, 1965–1974. [CrossRef]
27. Ikotun, J.; Adeyeye, R.; Otieno, M. Application of mine tailings sand as construction material—A review. *MATEC Web Conf.* **2022**, *364*, 05008. [CrossRef]
28. Reddy, R.B.M.; Satyanarayanan, K.S.; Jagannatha, H.N.; Parthasarathi, N. Use of Gold Mine Tailings in Production of Concrete—A Feasibility Study. *BDL* **2016**, *9*, 197–202.
29. Preethi, A.V.; Rajendra, S.; Navneeth, P.K.L. Studies on Gold Ore Tailings as Partial Replacement of Fine Aggregates in Concrete. *Int. J. Latest. Technol. Eng. Manag. Appl. Sci.* **2017**, *6*, 30–33. Available online: www.ijltemas.in (accessed on 2 September 2024).
30. Ahmed, T.; Elchalakani, M.; Basarir, H.; Karrech, A.; Sadrossadat, E.; Yang, B. Development of ECO-UHPC utilizing gold mine tailings as quartz sand alternative. *Clean. Eng. Technol.* **2021**, *4*, 100176. [CrossRef]
31. Balegamire, C.; Nkuba, B.; Dable, P. Production of gold mine tailings based concrete pavers by substitution of natural river sand in Misisi, Eastern Congo. *Clean. Eng. Technol.* **2022**, *7*, 100427. [CrossRef]
32. Song, Q.; Zou, Y.; Bao, J.; Zhang, P. Disposal of solid waste as building materials: A study on the mechanical and durability performance of concrete composed of gold tailings. *J. Mater. Res. Technol.* **2024**, *30*, 2111–2124. [CrossRef]
33. *SANS 1083:2014*; Aggregates from Natural Sources—Aggregate for Concrete. South African National Standard: Pretoria, South Africa, 2014.
34. *SANS 5845:2006*; Aggregate Tests—Bulk Density of Aggregate. South African National Standard: Pretoria, South Africa, 2006.
35. *SANS 5843:2008*; Water Absorption of Aggregates. South African National Standard: Pretoria, South Africa, 2008.
36. *SANS 50197-2:2011*; Cement Part 2: Conformity Evaluation. South African National Standard: Pretoria, South Africa, 2011.
37. *SANS 50450-1:2014*; Portland Cement Extenders. Part 1 Fly Ash; South African National Standard: Pretoria, South Africa, 2014.

38. *BS EN 934-2:2009*; Admixture for Concrete, Mortar and Grout. Concrete Admixtures. Definitions, Requirement, Conformity, Making and Labelling. British Standards Institution: London, UK, 2009.
39. Alexander, M.G.; Santhanam, M.; Ballim, Y. Durability design and specification for concrete structures—The way forward. *Int. J. Adv. Eng. Sci. Appl. Math.* **2010**, *2*, 95–105. [CrossRef]
40. *SANS 5861-1:2006*; Concrete Tests Part 1—Mixing Fresh Concrete in the Laboratory. South African National Standard: Pretoria, South Africa, 2006.
41. *SANS 5862-1:2006*; Concrete Tests Part 1—Consistence of Freshly Mixed Concrete—Slump Test. South African National Standard: Pretoria, South Africa, 2006.
42. *SANS 6250:2006*; Concrete Tests—Density of Compacted Freshly Mixed Concrete. South African National Standard: Pretoria, South Africa, 2006.
43. *SANS 5863:2006*; Concrete Tests—Compressive Strength of Hardened Cocnrete. South African National Standard: Pretoria, South Africa, 2006.
44. *SANS 6253:2006*; Concrete Tests—Tensile Splitting Strength of Concrete. South African National Standard: Pretoria, South Africa, 2006.
45. Alexander, M. *Durability Index Testing Procedure Manual, Ver 4.5.1*; University of Cape Town: Cape Town, South Africa, 2018; Volume 2018.
46. Charlaftis, D. Assessing Sandstone Reservoir Quality: Identifying the Reality. Doctoral Dissertation, Durham University, Durham, UK, 2021.
47. Zhou, H.M.; Qiao, X.C.; Yu, J.G. Influences of quartz and muscovite on the formation of mullite from kaolinite. *Appl. Clay Sci.* **2013**, *80*, 176–181. [CrossRef]
48. Cai, L.; Ma, B.; Li, X.; Lv, Y.; Liu, Z.; Jian, S. Mechanical and hydration characteristics of autoclaved aerated concrete (AAC) containing iron-tailings: Effect of content and fineness. *Constr. Build. Mater.* **2016**, *128*, 361–372. [CrossRef]
49. Mashifana, T.P. Beneficiation of Barberton Gold Mine Tailings: The Effect of Fly Ash on the Mineralogy and Micrograph. 2018. Available online: https://core.ac.uk/download/pdf/161412668.pdf (accessed on 2 September 2024).
50. Mufteeva, L.F.; Pavlova, I.A.; Farafontova, E.P. The effect of enrichment on quartz sand properties. *IOP Conf. Ser. Mater. Sci. Eng.* **2020**, *966*, 012027. [CrossRef]
51. Santander, M.; Valderrama, L. Recovery of pyrite from copper tailings by flotation. *J. Mater. Res. Technol.* **2019**, *8*, 4312–4317. [CrossRef]
52. Adiguzel, D.; Tuylu, S.; Eker, H. Utilization of tailings in concrete products: A review. *Constr. Build. Mater.* **2022**, *360*, 129574. [CrossRef]
53. Wang, L.; Shen, L.; Sun, W.; Ji, B.; Tang, H. The effects of natural weathering ages on mineralogical, physical, and chemical properties of stacking molybdenum tailings. *Environ. Sci. Pollut. Res.* **2022**, *29*, 87817–87827. [CrossRef] [PubMed]
54. Mueller, O.H. Some aspects of the effect of micaceous sand on concrete. *Civ. Eng. Siviele Ingenieurswese* **1971**, *1971*, 313–315.
55. Nosrati, A.; Addai-Mensah, J.; Skinner, W. Muscovite clay mineral particle interactions in aqueous media. *Powder Technol.* **2012**, *219*, 228–238. [CrossRef]
56. Sposito, R. Investigations on the Impact of Metaphyllosilicates and Calcined Common Clays on the Rheology and Early Hydration of Cements Admixed with Different Superplasticizers. Doctoral Dissertation, Universität der Bundeswehr München, Neubiberg, Germany, 2022.
57. Zografou, A.; Heath, A.; Walker, P. China clay waste as aggregate in alkali-activated cement mortars. *Proc. Inst. Civ. Eng. Constr. Mater.* **2014**, *167*, 312–322. [CrossRef]
58. Oritola, S.; Saleh, A.L.; Mohd Sam, A.R. Performance of Iron Ore Tailings as Partial Replacement for Sand in Concrete. *Appl. Mech. Mater.* **2015**, *735*, 122–127. [CrossRef]
59. Quan, X.; Wang, S.; Li, J.; Luo, J.; Liu, K.; Xu, J.; Zhao, N.; Liu, Y. Utilization of molybdenum tailings as fine aggregate in recycled aggregate concrete. *J. Clean. Prod.* **2022**, *372*, 133649. [CrossRef]
60. Thomas, B.S.; Damare, A.; Gupta, R.C. Strength and durability characteristics of copper tailing concrete. *Constr. Build. Mater.* **2013**, *48*, 894–900. [CrossRef]
61. Zhao, J.; Ni, K.; Su, Y.; Shi, Y. An evaluation of iron ore tailings characteristics and iron ore tailings concrete properties. *Constr. Build. Mater.* **2021**, *286*, 122968. [CrossRef]
62. Patil, M.V.; Patil, Y.D. Effect of copper slag and granite dust as sand replacement on the properties of concrete. *Mater. Today Proc.* **2020**, *43*, 1666–1677. [CrossRef]
63. Yang, J.; Wu, H.; Tang, Z.; Huo, X.; Lu, J.; Xu, L. Recycling spodumene flotation tailings in cement mortar: A synergy with metakaolin. In Proceedings of the 2011 International Conference on Computer Distributed Control and Intelligent Environmental Monitoring, Changsha, China, 19–20 February 2011; IEEE: Piscataway, NJ, USA, 2021; pp. 1687–1690. [CrossRef]
64. Shettima, A.U.; Hussin, M.W.; Ahmad, Y.; Mirza, J. Evaluation of iron ore tailings as replacement for fine aggregate in concrete. *Constr. Build. Mater.* **2016**, *120*, 72–79. [CrossRef]
65. Alexander, M.G.; Mackechnie, J.R.; Ballim, Y. *Guide to the Use of Durability Indexes for Achieving Durability in Concrete Structures*; Research Monograph No. 2; Department of Civil Engineering, University of Cape Town: Cape Town, South Africa, 1999.
66. Zhang, W.; Gu, X.; Qiu, J.; Liu, J.; Zhao, Y.; Li, X. Effects of iron ore tailings on the compressive strength and permeability of ultra-high performance concrete. *Constr. Build. Mater.* **2020**, *260*, 119917. [CrossRef]

67. Teggin, J.W. *Corrosion of Reinforcing Steel Induced by Combined Penetration of Chlorides and Carbon Dioxide in Concrete with Construction Cold Joints*; University of the Witwatersrand: Johannesburg, South Africa, 2022.
68. Ince, C. Reusing gold-mine tailings in cement mortars: Mechanical properties and socio-economic developments for the Lefke-Xeros area of Cyprus. *J. Clean. Prod.* **2019**, *238*, 117871. [CrossRef]
69. Siddique, S.; Jang, J.G. Assessment of molybdenum mine tailings as filler in cement mortar. *J. Build. Eng.* **2020**, *31*, 101322. [CrossRef]
70. Ghazi, A.B.; Jamshidi-Zanjani, A.; Nejati, H. Utilization of copper mine tailings as a partial substitute for cement in concrete construction. *Constr. Build. Mater.* **2022**, *317*, 125921. [CrossRef]
71. Pyo, S.; Tafesse, M.; Kim, B.J.; Kim, H.K. Effects of quartz-based mine tailings on characteristics and leaching behavior of ultra-high performance concrete. *Constr. Build. Mater.* **2018**, *166*, 110–117. [CrossRef]

Disclaimer/Publisher's Note: The statements, opinions and data contained in all publications are solely those of the individual author(s) and contributor(s) and not of MDPI and/or the editor(s). MDPI and/or the editor(s) disclaim responsibility for any injury to people or property resulting from any ideas, methods, instructions or products referred to in the content.